For submission to: W. A. Eaton Festschrift, JCP B

Cell Volume Controls Protein Stability and Compactness of the Unfolded State

Yuhan Wang,[1,*] Shahar Sukenik,[2,*,†] Caitlin Davis[2,3], and Martin Gruebele[1,2,3,†]

[1]Center for Biophysics and Computational Biology, University of Illinois, Urbana, Illinois, 61801, [2]Department of Chemistry, University of Illinois, Urbana, Illinois, 61801, and [3]Department of Physics, University of Illinois, Urbana, Illinois, 61801

Abstract

Macromolecular crowding is widely accepted as one of the factors that can alter protein stability, structure, and function inside cells. Less often considered is that crowding can be dynamic: as cell volume changes, either as a result of external duress or in the course of the cell cycle, water moves in or out through membrane channels, and crowding changes in tune. Both theory and *in vitro* experiments predict that protein stability will be altered as a result of crowding changes. Yet it is unclear how much the structural ensemble is altered as crowding changes in the cell. To test this, we look at the response of a FRET-labeled kinase to osmotically-induced volume changes in live cells. We examine both the folded and the unfolded states of the kinase by changing the temperature of the media surrounding the cell. Our data reveals that crowding compacts the structure of its unfolded ensemble but stabilizes the folded protein. We propose that the structure of proteins lacking a rigid, well defined tertiary structure could be highly sensitive to both increase and decrease in cell volume. Our findings present a possible mechanism for disordered proteins to act as sensors and actuators of cell cycle or external stress events that coincide with a change in macromolecular crowding.

Introduction

The interior of the cell, where most proteins perform their function, is heterogenous and dynamic. Proteins have evolved to perform optimally under the native crowded conditions that exist inside the cell.[1–4] Yet the idea of a constant, "native" cellular environment is at odds with the transient conditions often found in live cells. Even in multicellular organisms, cells change volume in the "rounding" process leading to mitosis[5,6], during metastasis[7] and blebbing[8], and as a result of shear forces[9] or while squeezing through tight junctions.[10,11] These morphological changes carry with them changes to the composition of abundant small solutes as well as larger biomolecules.[8,12–14] Such a change in the cellular environment can have dramatic effects in certain cases. For example, pioneering work by Eaton and co-workers[11,15] highlights how even small volume changes of erythrocytes can expedite the highly cooperative aggregation of mutated hemoglobin in sickle cells.

More recently, researchers have examined how cellular volume changes alter protein function in less cooperative processes. The fact that cellular volume is a highly tunable parameter, controllable by changes to external osmotic pressure, makes it convenient to use as a perturbation method to probe protein function inside the cell.[12,16–19] For example, cellular volume changes were shown to reduce protein stability[20] or alter complex concentrations formed by relatively weak protein-protein interactions in live cells.[12] In another example, volume oscillations were used to reveal the osmotic-stress mitigation mechanism in yeast cells,[16] or the role of the cell wall in *E. coli* cell growth.[17] This body of work complements numerous other studies comparing between protein stability in dilute solutions and in the crowded cellular interior.[21–25] Overall, the emerging picture highlights the remarkably heterogenous effect of the cellular milieu on protein stability.

Groundbreaking work by Minton and co-workers has shown that a crowded solution can increase protein stability by favoring a more compact state that takes up less space in solution.[2,26] The increased stability can be understood in terms of a shift towards higher melting temperature (T_m) – the temperature at which the population of a two-state protein is equally divided between its folded and unfolded state. This T_m shift increases the fraction of proteins in the folded state at a given temperature without changing the structure of the two states.[27,28] Since its inception, macromolecular crowding theory has been refined, and today it is understood that macromolecules can have both repulsive interactions with protein surfaces (mainly entropic) that often stabilize the native state of proteins, or sticking interactions (at least partly enthalpic) that could either stabilize or destabilize proteins,[29–31] depending on the protein's shape and electrostatic/hydrophobic

interactions of its surface with the surrounding solution.[32] These enthalpic, or "soft" interactions, can lead to unexpected consequences in the presence of macromolecular crowders.[33–36]

As one such example, there is accumulating evidence that the unfolded state is especially susceptible to structural changes that occur from crowded environments. Recent work shows how changes to crowded conditions induced by the addition of inert polymers such as Ficoll or dextran have a significantly larger effect on unfolded proteins than on folded ones.[37–39] Experiments by Pielak and co-workers have even highlighted this sensitivity in *E. coli* cells.[40] The importance of the unfolded state should not be underestimated: at any given moment, a non-negligible percentage of well-folded proteins is predicted to be unfolded, even when the cell is in optimal conditions.[41,42] If we account for intrinsically disordered proteins, which amount to roughly 30% of the human proteome,[43] a significant percentage of the proteome may be responsive to volume changes. Since such volume changes occur naturally, we wanted to test the sensitivity of a model protein under folding and unfolding conditions to crowding changes.

We use live cell microscopy to directly test the sensitivity of the unfolded state to crowding changes. We change in-cell crowding by controlling the media's osmotic pressure, and follow the fluorescence of a FRET labeled protein transiently expressed in cells to understand the effect of these changes on its structure. We use fPGK, a modified, active phosphoglycerate kinase that is conjugated with AcGFP1 and mCherry at the N- and C-terminus, respectively. The FRET signal from this fPGK has been shown to be a good proxy for its structure.[44–46] For this work, we use $fPGK_{LT}$, a low-melting temperature mutant of fPGK (sequence in **SI, Table S2**) that unfolds in the cell at ~ 35 ± 1 °C – a temperature where the cell is still viable. $fPGK_{LT}$, like other fPGK variants, exists in a pseudo two-state equilibrium inside cells (as indicated by a single transition between two end states detected by our experiment; strictly speaking PGK is a multi-state folder).[44] We tune the population distribution between these two states *in situ* by controlling the temperature of the cell's surrounding media. We then test the response of $fPGK_{LT}$ to cellular volume change by altering the osmotic pressure around the cells and measuring the average cellular FRET signal using epifluorescent microscopy. A reciprocal change in green and red fluorescence was previously shown to be indicative of a change in positioning between the two FRET labels – caused by a structural change in the protein.[44,47]

Our experiments show that the folded state of $fPGK_{LT}$ is not very susceptible to cellular volume changes: when $fPGK_{LT}$ populations are primarily folded, increasing or decreasing the cell's water

volume by up to 30% has little or no effect on protein compactness as judged by FRET. This makes sense because many enzymes, especially ones involved in crucial metabolic cycles, evolved to function well even when the cell itself is under duress.[48] As the surrounding media's temperature increases, an unfolded $fPGK_{LT}$ population emerges. Our experiments show that the FRET signal from this unfolded population is responsive to volume changes: decreasing cellular volume can compress the unfolded $fPGK_{LT}$, in a manner similar to that observed for other proteins due to macromolecular crowding.[49,50] Upon volume increase, the structure of $fPGK_{LT}$ further expands, indicating that the original unfolded population was not completely extended in the cell.[51,52] Our data shows that both increased and decreased cellular crowding induces conformational changes in the structure of the unfolded state.

The work shown here highlights the sensitivity of proteins to changes that can occur naturally or as a result of environmental stress in live cells, and indicates that more research should be done regarding how proteins act and interact in conditions that fluctuate around the optimum. Specifically, the unfolded state of proteins, or proteins that are primarily disordered, should be probed to see if function is altered or turned on/off when crowding in the cell is altered.

Methods

Plasmid design. The plasmid for the $fPGK_{LT}$ fusion construct was designed with an *in vitro* melting temperature of ~35 °C, so that the protein could be unfolded at temperatures where mammalian cells are viable. This mutant was designed based on an enzymatically active, less destabilized triple mutant (Y122W/W308F/W333F) of yeast PGK, $fPGK_{HT}$, with a melting temperature of ~42 °C.[45] To further destabilize the protein, we made the enzymatically active point mutations (F333W, P204H)[53] and loop insertion (89_90insSGGGGAG).[54] The protein was labeled at the N-terminus with AcGFP1 and the C-terminus with mCherry, with a two amino acid linker between the protein and the label. To assist with *in vitro* purification, a 6xHis-tag and thrombin cleavage site were added to the N-terminus of the AcGFP1. This gene was cloned between BamHI and NotI in the pDream 2.1 expression vector (GenScript Biotech), which has a CMV promoter for expression in mammalian cells.

Materials U-2 OS cells from ATCC were grown in DMEM supplemented with 10% FBS, 5% penicillin streptomycin and 5% sodium pyruvate in 75 cm^2 cell culture flasks. Imaging was done in FluoroBrite media (Gibco) supplemented with NaCl or diluted with MiliQ water. 40 mm round

#1.5 coverslips (Bioptechs) were cleaned by holding them to an open flame for 1 s, sonicating once in 1 M KOH for 10 minutes, twice in water for 10 minutes, and stored in 70% ethanol.

Transfection Cells were transfected using 10 μL Lipofectamine 2000 and 4 μg of the appropriate plasmid once the culture reached 70-80% confluence. After incubation in DMEM without penicillin streptomycin for 5 to 6 hours, cells were trypsinized and plated on precleaned 40 mm round #1.5 coverslips (Bioptechs) in dishes for 14 hours.

Flow cell microscopy All flow cell experiments were done using an FCS2 chamber (Bioptechs). This is a closed system with perfusion tubes for near laminar flow and temperature control, that can maintain constant temperature. The coverslip with adhered, transfected cells was washed twice with 2mL FluoroBrite media before being placed on a microaqueduct slide with a 100 μm thick 14 mm × 22 mm rectangular silicon gasket. The chamber was assembled locked, and connected to the flow system, making sure that there was no bubble in between the coverslip and microaqueduct slide. The FCS2 chamber was used to control temperature inside the flowcell by using a temperature controller. A second probe for the temperature, a J-type thermocouple, was inserted directly into the outlet tube of the FCS2 chamber. Temperatures measured from inlet tube and outlet tube has a difference less than 0.5 ℃. (**Fig. S1**)

Media reservoirs were placed in a water bath with temperature control to create a stable baseline for media temperature. All media lines were isolated with cotton and aluminum foil to reduce heat loss. Once the temperature in the flowcell equilibrated at the appropriate temperatures for 90 seconds, imaging was initiated. Initially isosmotic (0.3 Osm) media was flowed over the cells at a rate of 3 mL/min for 10 s. We then switched from the isosmotic reservoir to a non-isosmotic one by using a distributor (IDEX), and flowed this media for an additional 120 s at the same rate, before switching back to the isosmotic media. The flow rate was controlled using a nitrogen flow controlled by a piezo valve (Elveflow OB1), and coupled to a flow meter to adjust pressure in order to maintain a constant flow and prevent focus drift. A flow-related focus drift occurred when switching between reservoirs. A temperature-related focus drift occurred after switching since it took a few seconds for the FCS2 chamber to reach equilibrium. (**Movie S1**). The entire setup was timed and controlled using a home-built Labview program (National Instruments).

Fluorescence imaging was done by exciting the donor or the acceptor at 470 nm or 590 nm, respectively, using an LED (ThorLabs M470-L3, M590-L3). For FRET, following donor excitation, emitted light was split into green and red channels by a dichroic (Chroma), and directed on to adjacent spots on a Phantom V12.1 CMOS camera. Imaging was performed at 24 frames per

second with 800×600 resolution using a 63x NA 0.85 N-achroplan air-immersion objective (Zeiss). Our imaging shows that U-2 OS cells can survive in extreme hypoosmotic (~0.1 Osm) or hyperosmotic (~0.8 Osm) media, and can recover rapidly once the osmotic stress disappears (**Fig. S2**, **Movies S1** and **S2**).

Osmolarity calibration To determine the time dependence of osmolarity change during flow cell microscopy we rely on separate calibration experiments. Calibration experiments use one reservoir containing water, and the other reservoir containing water with 0.2 μM fluorescein. Imaging was performed in the same way as flow cell microscopy (see above). The rate of media switching is quantified by the changes in the fluorescein fluorescence signal, as shown in **Fig. S3**, and used to assess the switching between isosmotic and non-isosmotic media. To determine the calibration uncertainty, independent measurements were performed on different slides and different imaging positions on a single slide and showed good reproducibility (**Fig. S4**).

FReI experiments 25×75 mm^2, 1.0 mm thick slide (VMR) coverslips with adhered, transfected U-2 OS cells were attached to slides using 120 μm thick spacer sticker (Grace biolabs). The FReI microscope setup was described in previous works.[19,45,46] To obtain sharp stair-stepping temperatures (temperature jump, T-jump), a 2200 nm IR diode laser was focused on the imaged cells, which was heated rapidly by modulating the laser amplitude. Imaging was performed at 60 frames per second with 800×600 resolution using a 63× NA 0.85 N-achroplan air-immersion objective (Zeiss).

Data analysis MATLAB (MathWorks) was used to analyze all data. To quantify changes in protein structure resulting from osmotic modulation, we measured the fluorescence of both green and red channels. We examine the change in fluorescence before and after volume change, $\Delta F = F_{stress} - F_{iso}$, where subscript stress and iso denote the osmotically stressed or isosmotic signal, respectively. The fluorescence during imaging can be affected by bleaching, cell volume V change, temperature change and cross-talk between the two channels (**Eq. 1**)

$$\Delta F = \Delta F(V) + \Delta F(B) + \Delta F(T) + \Delta F(cross\ talk). \quad [1]$$

The three terms on the right hand side correspond to the change in fluorescence due to volume change $\Delta F(V)$, bleaching $\Delta F(B)$, and temperature change $\Delta F(T)$. The bleaching term $\Delta F(B)$ was corrected by subtracting a linear function fitted to the plateau after temperature equilibration. The temperature change correction is described in **Fig. S5**. The fluorescence changes as a result of

volume change are of main interested here. From this signal, the protein structural change can be assessed by D/A or relative FRET change χ (**Eq. 2** and **Eq. 3**). D/A was calculated by

$$D/A = \frac{F_{green}}{F_{red}}, \quad [2]$$

where, F_{red} and F_{green} are intensities of acceptor (mCherry) and donor (AcGFP). Relative FRET change was calculated by

$$\chi = \frac{S_{stress} - S_{iso}}{S_{iso}}, \quad [3]$$

where S_{stress} and S_{iso} are observed signals after and before osmotic challenge.

We assume that the water content of the cell, which is not taken up by large molecules such as other proteins, is initially 70% of the total volume[12,55,56]. We then estimate the change in free cellular volume upon osmotic duress, since the macromolecular content of the cell remains largely constant during short osmotic challenges.[4,18] We calculate the free volume (i.e. that not occupied by macromolecules) in the cell, V_f, following an osmotic challenge through **Eq. 4**:

$$V_f = 1 - \frac{1 - V/V_0}{0.7}, \quad [4]$$

where V_0 and V are the volume before and after osmotic challenge, respectively.[12] We calculate the change in relative cell volume by $\Delta V_f = (V_{f,\,stress} - V_{f,\,iso})$.

Results

Osmotic pressure correlates with cell volume change. In order to perturb the cell's volume, we use DMEM media supplemented with purified MiliQ water (for hypoosmotic conditions) or with NaCl (for hyperosmotic conditions) (**Fig. 1A**). We have previously quantified the relationship between cell volume change and media osmotic pressure by using fast 3D confocal microscopy to measure cell volume.[12] (**Fig.1B**) We use this relationship to report directly on the change of free volume (the volume not occupied by macromolecules) in the cell, rather than the external osmotic pressure. We do this by estimating the initial free volume (e.g. the volume occupied by water in the cell) of ~ 70%, and attribute any changes in total volume changes to this free volume (**Eq. 4**). This is rationalized by the fact that water moves in and out of the cell orders of magnitude faster than even small solutes.[57]

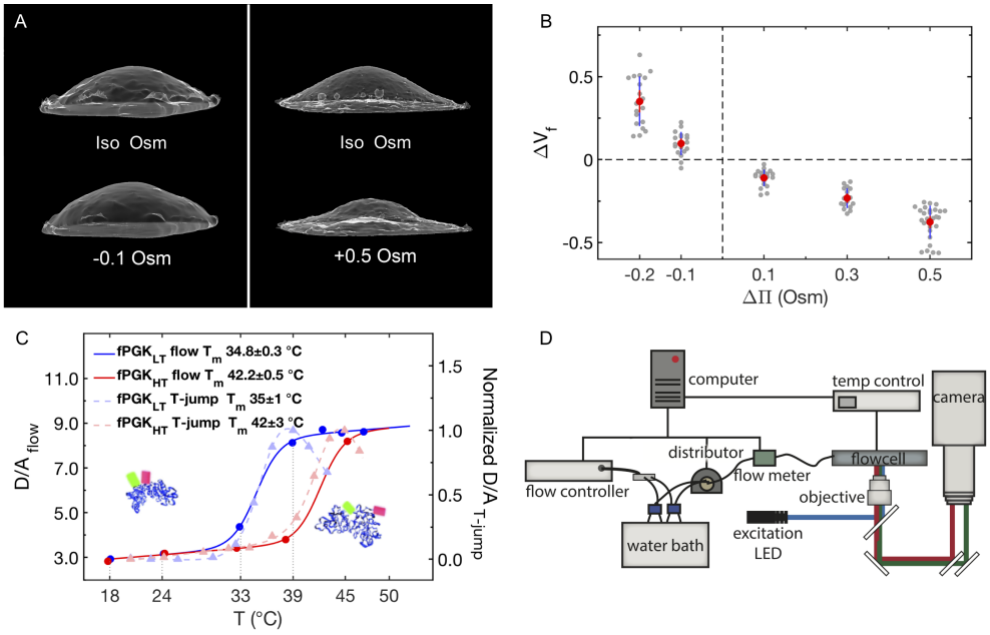

Figure 1. Volume modulation and protein response. (A) 3D reconstruction of confocal images of cell surfaces before (top) and after (bottom) -0.1 Osm (left) or +0.5 Osm (right) change. (B) Relative free water volume change ΔV_f as a function of osmolarity change. (C) In-cell D/A of $fPGK_{LT}$ and $fPGK_{HT}$ measured by volume modulation or T-jump as a function of temperature. In-cell temperature was obtained by temperature calibration as described in **Fig. S6**. The majority of $fPGK_{LT}$ was folded at 18 °C and 24 °C (left structure), the unfolded population increased at 33 °C and nearly the entire protein was unfolded at 39 °C (right structure). (D) Schematic of volume-modulation setup, as detailed in Methods.

Controlling the partitioning of $fPGK_{LT}$ between the folded and unfolded state. We use temperature to tune how the cellular $fPGK_{LT}$ population is distributed between the folded and unfolded states. The in-cell melting temperature (T_m) of $fPGK_{LT}$ was measured by the FReI experiment (**Methods**). Similar to what was reported previously for a higher T_m PGK mutant ($fPGK_{HT}$, T_m = 42 ± 1 °C, **Fig. 1C**), $fPGK_{LT}$ melting shows a characteristic sigmoid shape, with the midpoint at 35±1°C (**Fig. 1C**). Below this point, the baseline represents a population that is largely folded. Above this point, the baseline represents a population that is largely unfolded. We picked temperatures below (18 °C, 24 °C), around (33 °C) and above (39 °C) the melting temperature to change the ratio between folded and unfolded $fPGK_{LT}$ populations. We use a microscope setup equipped with a flowcell and temperature control (**Fig. 1D**) to modulate crowded conditions in the cell through changes to media osmotic pressure. The readout temperature was calibrated by measuring the T_m of $fPGK_{LT}$ and $fPGK_{HT}$, as described in **Fig. S6**.

Representative experiments at low and high temperature, as cell volume decreases, are shown together with control experiments where the volume is not changed in **Fig. 2**. Throughout the

experiment, the surface area of the cell remains constant (**Fig. 2A**), meaning the volume loss occurs primarily in cell-height loss, as previously reported.[12,19] In experiments where the media remained isosmotic after the switch, no change was observed in green or red fluorescence (**Fig. 2B-E, 1st and 3rd column**). A signal change is observed only when hypo/hyperosmotic media was flowed over the cell, decreasing its volume (**Fig. 2B-E, 2nd and 4th column**). In all cases except high temperature and volume change,[19] the return to basal volume causes complete recovery of the fluorescence signal to their original levels, indicative of a highly reversible structural change induced by volume changes.

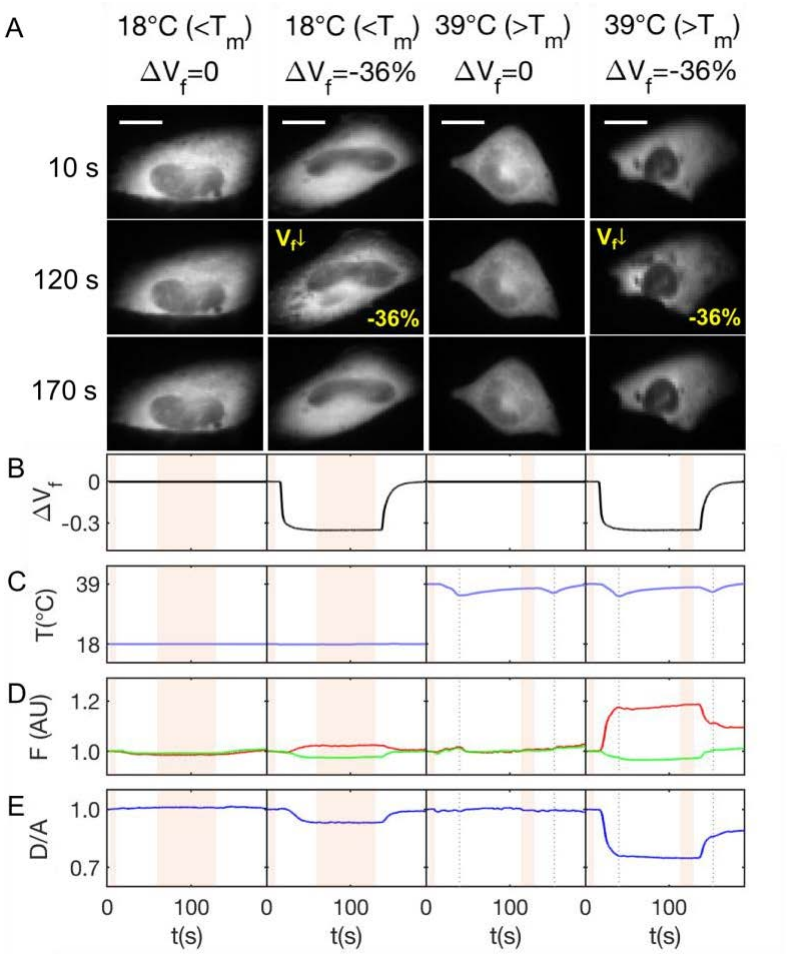

Figure 2. fPGK$_{LT}$ in U-2 OS cells responds to cell volume modulation. (A) micrographs of U2-OS cells before (top) , during (middle), and after recovery (bottom) of volume changes. Relative volume change ΔV_f are written at the bottom right hand side. Volume changes were calculated based on media osmolarity (**Fig. 1B**, **Fig. S3**) The temperature and volume change of all cells are specified in at the top of each column. Scale bars are 10 µm. (B) Relative free cell volume change as a function of time. Switching occurs at 10 and 130 s. (C) Temperature measured by thermocouple at the outlet of the FCS2 chamber. The dips in temperature seen at 39 ℃ at ~ 40 and ~ 150 s are a result of flow switching. We correct for this artifact as described in **Fig. S5** and **Table S1**. (D) Whole-cell averaged green and red fluorescence intensity normalized to their initial values. (E) FRET signal normalized to initial values.

Free cell volume changes perturb unfolded, but not folded fPGK$_{LT}$ structure. To understand how volume changes affect the different structural ensembles of fPGK$_{LT}$, we performed volume modulation experiments below, around and above the T_m and follow the change in green and red fluorescence that occurred as a result (**Fig. 3**). We first noted that when the cells are at room temperature (18°C, **Fig. 3 left column**) and the majority of fPGK$_{LT}$ is in the folded population (as indicated by the in-cell melting curve in **Fig. 1D**), little change occurs in both red and green fluorescence as the cell volume is reduced. Slightly larger, but still small, is the change in green and red fluorescence when the cell volume increases. Increasing the temperature to 24 °C shows a slight increase in the amplitude at the largest and smallest volume conditions, but an overall small change is shown.

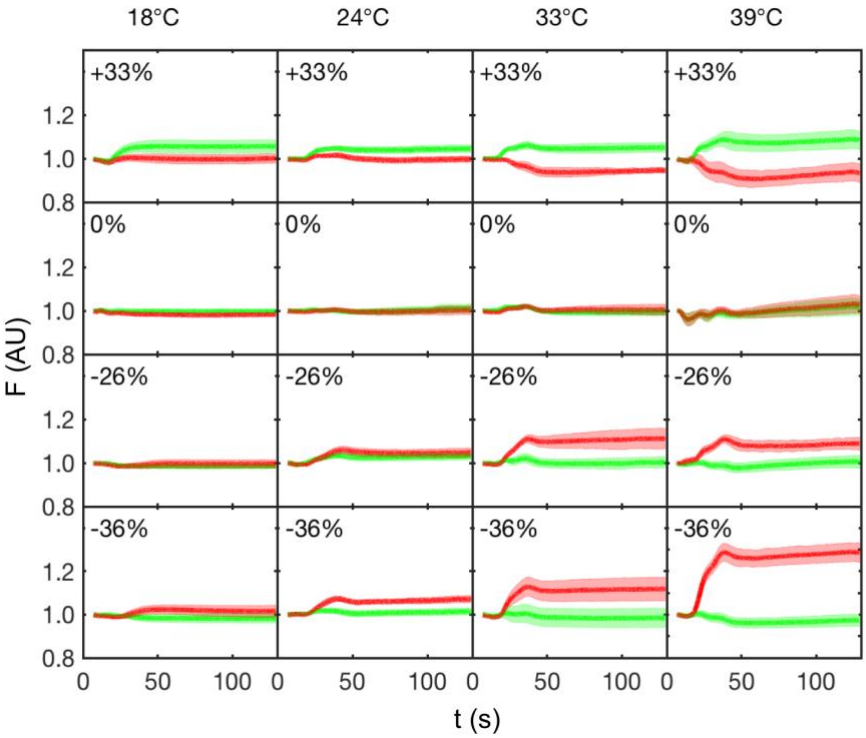

Figure 3. Green and red fluorescence changes due to volume modulation below, around, and above the melting temperature after temperature correction. Fluorescence is normalized to isosmotic period averaged between 4 and 10 seconds after we start imaging. Temperature is specified at the top of each column, and volume change is specified at the top of each panel. Solid lines are means of between 7 and 21 experiments from at least 4 separate transfections. Shaded areas are SD of repeats. More details and data before corrections are shown in **Fig. S4**.

As the temperature increases further to 33 °C, the amplitude upon volume perturbation of both green and red fluorescence grows significantly. This coincides with the onset of unfolding, as shown in **Fig. 1C**. At this temperature, the protein population is estimated to be 20±10 % unfolded. The change in green and red fluorescence becomes even larger at 39 °C, when nearly the entire

protein population is unfolded. Notably, the green fluorescence changes are smaller than the red. This may be explained by (1) The fact that we are considering a relative change, and that the absorption and fluorescence quantum yield of AcGFP1 are significantly greater than those of mCherry,[58] and (2) the fact that not all proteins contain both tags: Since the donor is at the N-terminal of the protein, incomplete expression or subsequent cleavage would create a donor-only construct. A donor-only fPGK (or just monomeric GFP) population is not expected to change its fluorescence signal even when structural changes occur in its protein conjugate since there is no acceptor for FRET; as such, this population acts to reduce the overall change in fluorescence seen signal seen in **Fig. 3**.

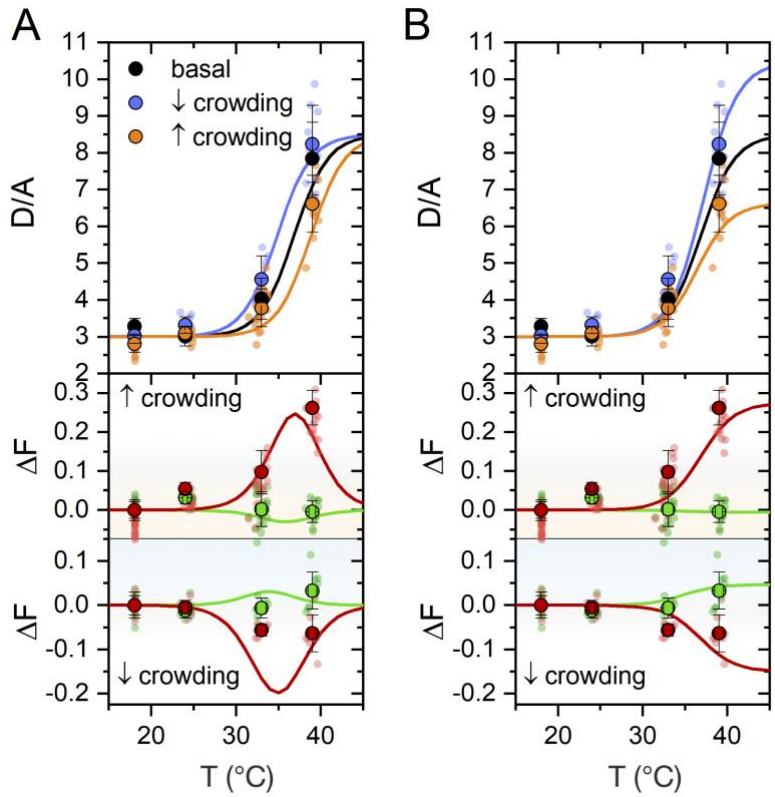

Figure 4. T_m shift vs unfolded restructuring. (**A**) T_m shift or (**B**) change in unfolded compactness a result of crowding are shown for a parameter-free model (lines) and for data from Fig. 3 (large symbols are averages of all individual cells, shown as smaller, semi-transparent symbols.). Error bars are SD of the data. Our model assumes a sigmoidal dependence of folded population on temperature, with a basal midpoint of 35 ℃, and a decay constant of 2 ℃. The green and red fluorescence is then calculated in crowding increase (middle panel) and decrease (bottom panel). The ΔF values correspond to change in fluorescence based on the folded ensemble. These are calculated using basal values for folded (1500, 500 AU for green and red, respectively) and unfolded conformation (1700, 200 AU for green and red, respectively). For (A), Tm shift is ±2℃, as estimated from experiments in Ficoll.[25] For (B) there was no T_m shift. Instead, the unfolded state green and red fluorescence was varied by ±15%, as indicated from experiments at high temperatures.

One key observation is the sensitivity of the unfolded ensemble to crowding decrease. Little attention has been paid to the fact that volume increase through water influx, a process that occurs routinely in the cell cycle[5,6,59], carries with it a reduction in crowded conditions. We find that the folded state remains fairly insensitive to decrease in crowded conditions, as noted by the small fluorescence changes at 18 and 24°C. This is not surprising: the folded state is held together tightly by thousands of non-covalent interactions, and we do not expect large conformational changes resulting from decreased crowding. The unfolded state, however, has been shown to display more flexibility *in vitro* as well.[40,50,60]

Discussion

The signal changes shown in **Fig. 3** can be explained by two scenarios. In one scenario, which we term "T_m shift" scenario, the protein coexists between a folded and an unfolded ensemble with lower and higher D/A ratios, respectively. As crowding changes, protein population is redistributed, and the change in fluorescence is a result of this distribution. Such redistribution essentially amounts to a shift in melting temperature T_m, and does not involve structural change in the ensembles. Indeed, we recently showed that in the presence of increasing concentration of the polymeric crowder Ficoll, the T_m of fPGK increases.[25] This is shown in **Fig. 4A, top**. The other scenario, which we term "change in unfolded compactness", attributes the change in fluorescence to compaction or expansion of the unfolded state. In this scenario, the T_m may remain constant, as shown for the latter in **Fig. 4B, top**.

To differentiate between the 'T_m shift' and the 'change in unfolded compactness' scenarios, we calculate the fluorescence change for both in **Fig. 4**. We use characteristic values of green and red fluorescence for the folded and unfolded states (as obtained from **Fig. 1C**) as input. The estimated change in fluorescence as a result of a T_m (stability) shift due to a crowding increase (volume decrease) is shown in **Fig. 4A** (**middle**), and due to a crowding decrease (volume increase) in **Fig. 4A** (**bottom**). A prominent feature of the crowding-induced change in fluorescence, ΔF, is a peak that rises near the T_m. We show analogous simulations due to changes in unfolded state compactness in **Fig. 4B**. For this scenario, ΔF continues to increase with temperature until it plateaus. In both cases, crowding changes at low temperatures have no effect on the change in fluorescence. Not shown is a scenario where native state compactness changes, which would result in fluorescence changes at low temperature that are clearly not observed in our experiments.

For the case of crowding increase, we cannot rule out either scenario without additional data taken at even higher temperatures which are difficult to perform in live cells. For the case of crowding decrease (volume increase), however, we do not observe a peak in the green nor red fluorescence changes under our in-cell conditions. The experimental data (**symbols in Fig. 4**) instead shows a plateau at high temperature, and no effect at low temperature. Thus the 'change in unfolded compactness' best matches volume decrease experiments, whereas the shift in stability or native state compactness must make smaller contributions. We also mention the possibility of other scenarios, such as a destabilization of the unfolded state under increased crowding recently observed by Cohen and Pielak using NMR.[40] Due to the low resolution provided by our FRET experiments our data doesn't definitively support any one scenario.

Thus our model does not rule out small contributions from stability or native state compactness that occur simultaneously: a small shift of T_m (< 2 °C) would result in a peak contribution to the fluorescence curve that is overwhelmed by the plateau due to unfolded state compactness. Alternatively, a large T_m shift towards increased stability would results in a monotonic increase in fluorescence change over the temperature range we used. Changes in the native or unfolded baselines of the melting curve may also carry with them a range of behaviors that we did not account for. Finally, we do not account for possible changes in the cooperativity of the unfolding transition, which would alter the slopes of the curves seen in the top panel of **Fig. 4A, B**. All these factors can, individually or together, improve the fit of the experimental data to the simulated curves. Nonetheless, our model can rule out certain possibilities. Upon decreased crowding, the peak in ΔF occurs at lower temperatures than the original T_m if the effect is due to protein stability – this is certainly not observed, and so for decreased crowding there is no significant shift of protein stability in the cells (**Fig. 4A, bottom**). In addition, we can rule out significant structural changes of the folded state when crowding changes. In the case of structural change in the folded state, changes to green and red fluorescence would be noticeable at low temperature as well. Such changes are not observed, as shown in **Fig. 3**.

Our interpretation of the data shows that while additional crowding can compact the unfolded protein's structure, decreased crowding has a similar but opposite effect, causing the unfolded protein's structure to further expand. This implies that the unfolded protein is slightly collapsed even when the population is unfolded. This collapsed state responds to changes in crowding as predicted by entropic crowding forces, and demonstrated *in vitro* for both intrinsically disordered

proteins[50] and for expanded polymers.[61] An alternative explanation is that the unfolded protein contains some residual structure even at temperatures well past T_m. This residual structure can be compacted by an increase of cellular crowding, as expected for an extended conformation.[62,63] While these two cases cannot be differentiated by our experiments, our data implies that for PGK, the interactions holding these structures together are weak and driven by crowding, and not by "sticking" of the unfolded state to the cytoplasmic matrix.

Concluding remarks

This work highlights the dynamic nature of the unfolded state inside cells. Our experiments suggest that the unfolded state of proteins may be sensitive to changes in the cellular conditions that result from either routine cell cycle events or environmental duress. Such modulation of expanded protein structure would be particularly relevant for certain intrinsically disordered proteins that are known to contain residual structure.[49,64] We suggest that intrinsically disordered proteins could be possible sensors and actuators of cellular phenotype upon change in volume and/or crowding. Changes in cell volume are relevant even in the case of multi-cellular organisms, which generally maintain a constant osmotic pressure environment, due to natural processes that cause cell volume changes such as entry into mitosis or shape changes during cell motility.

In most cases, proteins are perturbed *in vitro* by changing temperature or pressure, adding denaturants or stabilizers, or titrating a drug or a binding partner. The *in vitro* solution conditions in these cases can always be well-controlled, and because of this the etiology of the observed effect can usually be traced to the perturbation performed.[31] Here, we use perturbations that are routinely done *in vitro*, but perform them in cells. The response of the fPGK protein probe to these perturbations integrates the physical-chemical effects that would occur in an aqueous solution, with the additional responses of the cell that are, to a large degree, unknown. To minimize at least the adaptive response (e.g. transcription up-regulation upon stress) of the cell to osmotic or temperature stress, our experiments are kept short, on the order of 2 to 3 minutes. In this time span, regulatory transcription is kept to a minimum, and the macromolecular components of the cell do not change dramatically in their organization.

Of course, we cannot rule out that secondary effects due to changes in the cytoplasmic matrix beyond volume, such as changing interactions of non-labeled species such as ions and other metabolites with our model protein, which can affect the measurements.[19] Indeed, recent work by

our group and others points to the importance of abundant small solutes including ions and ATP in determining protein structure and interactions.[19,24,65] Despite these currently unknown factors, this study presents ample evidence that cell volume changes could be an important contributor to protein structure and function, and especially the function of intrinsically disordered proteins.[52,66,67]

Supporting Information

Acknowledgments

This work was supported by NSF grant MCB 1803786. CMD was supported by a Fellowship from the Center for Physics in Living Cells, NSF PHY 1430124.

References

(1) Ellis, R. J.; Minton, A. P. Join the Crowd. *Nature* **2003**, *425*, 27–28.

(2) Minton, A. P. How Can Biochemical Reactions within Cells Differ from Those in Test Tubes? *J. Cell Sci.* **2006**, *119*, 2863–2869.

(3) Ebbinghaus, S.; Gruebele, M. Protein Folding Landscapes in the Living Cell. *J. Phys. Chem. Lett.* **2011**, *2*, 314–319.

(4) van den Berg, J.; Boersma, A. J.; Poolman, B. Microorganisms Maintain Crowding Homeostasis. *Nat. Rev. Microbiol.* **2017**, *15*, 309–318.

(5) Boucrot, E.; Kirchhausen, T. Mammalian Cells Change Volume during Mitosis. *PLoS One* **2008**, *3*, 1–3.

(6) Son, S.; Kang, J. H.; Oh, S.; Kirschner, M. W.; Mitchison, T. J.; Manalis, S. R. Resonant Microchannel Volume and Mass Measurements Show That Suspended Cells Swell during Mitosis. *J. Cell Biol.* **2015**, *211*, 757–763.

(7) Kim, D.-H.; Li, B.; Si, F.; Phillip, J. M.; Wirtz, D.; Sun, S. X. Volume Regulation and Shape Bifurcation in the Cell Nucleus. *J. Cell Sci.* **2015**, *128*, 3375–3385.

(8) Taloni, A.; Kardash, E.; Salman, O. U.; Zapperi, S.; Porta, C. A. M. La. Volume Changes during Active Shape Fluctuations in Cells. *Phys. Rev. Lett.* **2015**, *114*, 1–12.

(9) Heo, J.; Sachs, F.; Wang, J.; Hua, S. Z. Shear-Induced Volume Decrease in MDCK Cells. *Cell. Physiol. Biochem.* **2012**, *30*, 395–406.

(10) Eaton, W. A.; Hofrichter, J. The Biophysics of Sickle-Cell Hydroxyurea Therapy. *Science* **1995**, *268*, 1142–1143.

(11) Li, Q.; Henry, E. R.; Hofrichter, J.; Smith, J. F.; Cellmer, T.; Dunkelberger, E. B.; Metaferia, B. B.; Jones-Straehle, S.; Boutom, S.; Christoph, G. W.; et al. Kinetic Assay Shows That Increasing Red Cell Volume Could Be a Treatment for Sickle Cell Disease. *Proc. Natl. Acad. Sci. U. S. A.* **2017**, *114*, E689–E696.

(12) Sukenik, S.; Ren, P.; Gruebele, M. Weak Protein–protein Interactions in Live Cells Are Quantified by Cell-Volume Modulation. *Proc. Natl. Acad. Sci.* **2017**, *114*, 6776–6781.

(13) Burg, M. B.; Kwon, E. D.; Kültz, D. Regulation of Gene Expression by Hypertonicity. *Annu. Rev. Physiol.* **1997**, *59*, 437–455.

(14) Strange, K. Cellular Volume Homeostasis. *Adv. Physiol. Educ.* **2004**, *28*, 155–159.

(15) Christoph, G. W.; Hofrichter, J.; Eaton, W. A. Understanding the Shape of Sickled Red Cells. *Biophys. J.* **2005**, *88*, 1371–1376.

(16) Mitchell, A.; Wei, P.; Lim, W. A. Oscillatory Stress Stimulation Uncovers an Achilles Heel of the Yeast MAPK Signaling Network. *Science* **2015**, *350*, 1379–1383.

(17) Rojas, E.; Theriot, J. A.; Huang, K. C. Response of Escherichia coli Growth Rate to Osmotic Shock. *Proc. Natl. Acad. Sci. U. S. A.* **2014**, *111*, 7807–7812.

(18) Boersma, A. J.; Zuhorn, I. S.; Poolman, B. A Sensor for Quantification of Macromolecular Crowding in Living Cells. *Nat. Methods* **2015**, *12*, 227–230.

(19) Sukenik, S.; Salam, M.; Wang, Y.; Gruebele, M. In-Cell Titration of Small Solutes Controls Protein Stability and Aggregation. *J. Am. Chem. Soc.* **2018**, *140*, 10497–10503.

(20) Stadmiller, S. S.; Gorensek-Benitez, A. H.; Guseman, A. J.; Pielak, G. J. Osmotic Shock Induced Protein Destabilization in Living Cells and Its Reversal by Glycine Betaine. *J. Mol. Biol.* **2017**, *429*, 1155–1161.

(21) Schlesinger, A. P.; Wang, Y.; Tadeo, X.; Millet, O.; Pielak, G. J. Macromolecular Crowding Fails To Fold a Globular Protein in Cells. *J. Am. Chem. Soc.* **2011**, *133*, 8082–8085.

(22) Gnutt, D.; Gao, M.; Brylski, O.; Heyden, M.; Ebbinghaus, S. Excluded-Volume Effects in Living Cells. *Angew. Chemie Int. Ed.* **2015**, *54*, 2548–2551.

(23) Gnutt, D.; Brylski, O.; Edengeiser, E.; Havenith, M.; Ebbinghaus, S. Imperfect Crowding Adaptation of Mammalian Cells towards Osmotic Stress and Its Modulation by Osmolytes. *Mol. Biosyst.* **2017**, *13*, 2218–2221.

(24) Mu, X.; Choi, S.; Lang, L.; Mowray, D.; Dokholyan, N. V.; Danielsson, J.; Oliveberg, M. Physicochemical Code for Quinary Protein Interactions in *Escherichia coli*. *Proc. Natl. Acad. Sci.* **2017**, *114*, E4556-E4563.

(25) Davis, C. M.; Gruebele, M. Non-steric Interactions Predict the Trend and Steric Interactions the Offset of Protein Stability in Cells. *ChemPhysChem* **2018**, *45*, 669–676.

(26) Zhou, H.-X.; Rivas, G.; Minton, A. P. Macromolecular Crowding and Confinement: Biochemical, Biophysical, and Potential Physiological Consequences. *Annu. Rev. Biophys.* **2008**, *37*, 375–397.

(27) Wang, Y.; Sarkar, M.; Smith, A. E.; Krois, A. S.; Pielak, G. J. Macromolecular Crowding and Protein Stability. *J. Am. Chem. Soc.* **2012**, *134*, 16614–16618.

(28) Miklos, A. C.; Sarkar, M.; Wang, Y.; Pielak, G. J. Protein Crowding Tunes Protein Stability. *J. Am. Chem. Soc.* **2011**, *133*, 7116–7120.

(29) Sukenik, S.; Sapir, L.; Harries, D. Balance of Enthalpy and Entropy in Depletion Forces. *Curr. Opin. Colloid Interface Sci.* **2013**, *18*, 495–501.

(30) Benton, L. A.; Smith, A. E.; Young, G. B.; Pielak, G. J. Unexpected Effects of

Macromolecular Crowding on Protein Stability. *Biochemistry* **2012**, *51*, 9773–9775.

(31) Rivas, G.; Minton, A. P. Toward an Understanding of Biochemical Equilibria within Living Cells. *Biophys. Rev.* **2018**, *10*, 241–253.

(32) Sukenik, S.; Sapir, L.; Gilman-Politi, R.; Harries, D. Diversity in the Mechanisms of Cosolute Action on Biomolecular Processes. *Faraday Discuss.* **2013**, *160*, 225-237.

(33) Monteith, W. B.; Cohen, R. D.; Smith, A. E.; Guzman-Cisneros, E.; Pielak, G. J. Quinary Structure Modulates Protein Stability in Cells. *Proc. Natl. Acad. Sci.* **2015**, *112*, 1739–1742.

(34) Cohen, R. D.; Guseman, A. J.; Pielak, G. J. Intracellular PH Modulates Quinary Structure. *Protein Sci.* **2015**, *24*, 1748–1755.

(35) Sapir, L.; Harries, D. Is the Depletion Force Entropic? Molecular Crowding beyond Steric Interactions. *Curr. Opin. Colloid Interface Sci.* **2015**, *20*, 3–10.

(36) Sapir, L.; Harries, D. Origin of Enthalpic Depletion Forces. *J. Phys. Chem. Lett.* **2014**, *5*, 1061–1065.

(37) Mikaelsson, T.; Adén, J.; Johansson, L. B.-Å.; Wittung-Stafshede, P. Direct Observation of Protein Unfolded State Compaction in the Presence of Macromolecular Crowding. *Biophys. J.* **2013**, *104*, 694–704.

(38) Hong, J.; Gierasch, L. M. Macromolecular Crowding Remodels the Energy Landscape of a Protein by Favoring a More Compact Unfolded State. *J. Am. Chem. Soc.* **2010**, *132*, 10445–10452.

(39) Aznauryan, M.; Delgado, L.; Soranno, A.; Nettels, D.; Huang, J.; Labhardt, A. M.; Grzesiek, S.; Schuler, B. Comprehensive Structural and Dynamical View of an Unfolded Protein from the Combination of Single-Molecule FRET, NMR, and SAXS. *Proc. Natl. Acad. Sci.* **2016**, *113*, E5389–E5398.

(40) Cohen, R. D.; Pielak, G. J. Quinary Interactions with an Unfolded State Ensemble. *Protein Sci.* **2017**, *26*, 1698–1703.

(41) Ghosh, K.; Dill, K. Cellular Proteomes Have Broad Distributions of Protein Stability. *Biophys. J.* **2010**, *99*, 3996–4002.

(42) Lepock, J. R. Measurement of Protein Stability and Protein Denaturation in Cells Using Differential Scanning Calorimetry. *Methods* **2005**, *35*, 117–125.

(43) Wright, P. E.; Dyson, H. J. Intrinsically Disordered Proteins in Cellular Signalling and Regulation. *Nat. Rev. Mol. Cell Biol.* **2015**, *16*, 18–29.

(44) Dhar, A.; Samiotakis, A.; Ebbinghaus, S.; Nienhaus, L.; Homouz, D.; Gruebele, M.; Cheung, M. S. Structure, Function, and Folding of Phosphoglycerate Kinase Are Strongly Perturbed by Macromolecular Crowding. *Proc. Natl. Acad. Sci.* **2010**, *107*, 17586–17591.

(45) Ebbinghaus, S.; Dhar, A.; McDonald, J. D.; Gruebele, M. Protein Folding Stability and Dynamics Imaged in a Living Cell. *Nat. Methods* **2010**, *7*, 319–323.

(46) Dhar, A.; Gruebele, M. Fast Relaxation Imaging in Living Cells. *Curr. Protoc. protein Sci.* **2011**, *65,* 28.1.1-28.1.19.

(47) Guo, M.; Xu, Y.; Gruebele, M. Temperature Dependence of Protein Folding Kinetics in Living Cells. *Proc. Natl. Acad. Sci. U. S. A.* **2012**, *109*, 17863–17867.

(48) Neidleman, S. L. Enzyme Reactions under Stress Conditions. *Crit. Rev. Biotechnol.* **1989**, *9*, 273–286.

(49) Uversky, V. N. Intrinsically Disordered Proteins and Their Environment: Effects of Strong Denaturants, Temperature, PH, Counter Ions, Membranes, Binding Partners, Osmolytes, and Macromolecular Crowding. *Protein J.* **2009**, *28*, 305–325.

(50) Soranno, A.; Koenig, I.; Borgia, M. B.; Hofmann, H.; Zosel, F.; Nettels, D.; Schuler, B. Single-Molecule Spectroscopy Reveals Polymer Effects of Disordered Proteins in Crowded Environments. *Proc. Natl. Acad. Sci.* **2014**, *111*, 4874–4879.

(51) Meng, W.; Luan, B.; Lyle, N.; Pappu, R. V.; Raleigh, D. P. The Denatured State Ensemble Contains Significant Local and Long-Range Structure under Native Conditions: Analysis of the N-Terminal Domain of Ribosomal Protein L9. *Biochemistry* **2013**, *52*, 2662–2671.

(52) Tompa, P. The Interplay between Structure and Function in Intrinsically Unstructured Proteins. *FEBS Lett.* **2005**, *579*, 3346–3354.

(53) McHarg, J.; Kelly, S. M.; Price, N. C.; Cooper, A.; Littlechild, J. A. Site-Directed Mutagenesis of Proline 204 in the "hinge" Region of Yeast Phosphoglycerate Kinase. *Eur. J. Biochem.* **1999**, *259*, 939–945.

(54) Collinet, B.; Garcia, P.; Minard, P.; Desmadril, M. Role of Loops in the Folding and Stability of Yeast Phosphoglycerate Kinase. *Eur. J. Biochem.* **2001**, *268*, 5107–5118.

(55) Yancey, P. H. Water Stress, Osmolytes and Proteins. *Integr. Comp. Biol.* **2001**, *41*, 699–709.

(56) Record Jr, M. T.; Courtenay, E. S.; Cayley, D. S.; Guttman, H. J. Responses of E. coli to Osmotic Stress: Large Changes in Amounts of Cytoplasmic Solutes and Water. *Trends Biochem. Sci.* **1998**, *23*, 143–148.

(57) Jiang, H.; Sun, S. X. Cellular Pressure and Volume Regulation and Implications for Cell Mechanics. *Biophys. J.* **2013**, *105*, 609–619.

(58) Cranfill, P. J.; Sell, B. R.; Baird, M. A.; Allen, J. R.; Lavagnino, Z.; de Gruiter, H. M.; Kremers, G.-J.; Davidson, M. W.; Ustione, A.; Piston, D. W. Quantitative Assessment of Fluorescent Proteins. *Nat. Methods* **2016**, *13*, 557–562.

(59) Stewart, M. P.; Helenius, J.; Toyoda, Y.; Ramanathan, S. P.; Muller, D. J.; Hyman, A. A. Hydrostatic Pressure and the Actomyosin Cortex Drive Mitotic Cell Rounding. *Nature* **2011**, *469*, 226–230.

(60) Hofmann, H.; Soranno, A.; Borgia, A.; Gast, K.; Nettels, D.; Schuler, B. Polymer Scaling Laws of Unfolded and Intrinsically Disordered Proteins Quantified with Single-Molecule Spectroscopy. *Proc. Natl. Acad. Sci.* **2012**, *109*, 16155–16160.

(61) Kang, H.; Yoon, Y. G.; Thirumalai, D.; Hyeon, C. Confinement-Induced Glassy Dynamics in a Model for Chromosome Organization. *Phys. Rev. Lett.* **2015**, *115*, 1–5.

(62) Kohn, J. E.; Millett, I. S.; Jacob, J.; Zagrovic, B.; Dillon, T. M.; Cingel, N.; Dothager, R. S.; Seifert, S.; Thiyagarajan, P.; Sosnick, T. R.; et al. Random-Coil Behavior and the Dimensions of Chemically Unfolded Proteins. *Proc. Natl. Acad. Sci. U. S. A.* **2004**, *101*, 12491–12496.

(63) Riback, J. A.; Bowman, M. A.; Zmyslowski, A. M.; Knoverek, C. R.; Jumper, J. M.;

Hinshaw, J. R.; Kaye, E. B.; Freed, K. F.; Clark, P. L.; Sosnick, T. R. Innovative Scattering Analysis Shows That Hydrophobic Disordered Proteins Are Expanded in Water. *Science* **2017**, *358*, 238–241.

(64) Kuznetsova, I.; Turoverov, K.; Uversky, V. N. What Macromolecular Crowding Can Do to a Protein. *Int. J. Mol. Sci.* **2014**, *15*, 23090–23140.

(65) Patel, A.; Malinovska, L.; Saha, S.; Wang, J.; Alberti, S.; Krishnan, Y.; Hyman, A. A. ATP as a Biological Hydrotrope. *Science* **2017**, *356*, 753–756.

(66) Arai, M.; Sugase, K.; Dyson, H. J.; Wright, P. E. Conformational Propensities of Intrinsically Disordered Proteins Influence the Mechanism of Binding and Folding. *Proc. Natl. Acad. Sci.* **2015**, *112*, 9614–9619.

(67) Wicky, B. I. M.; Shammas, S. L.; Clarke, J. Affinity of IDPs to Their Targets Is Modulated by Ion-Specific Changes in Kinetics and Residual Structure. *Proc. Natl. Acad. Sci.* **2017**, *114*, 9882–9887.

TOC Graphic: